$Na_3[Ti_2P_2O_{10}F]$: A New Oxyfluorinated Titanium Phosphate with an Ionic Conductive Property

Sihai Yang,[†] Guobao Li,*[,†] Liping You,[‡] Julian Tao,[§] Chun-K. Loong,[§] Shujian Tian,[†] Fuhui Liao,[†] and Jianhua Lin*[,†]

Beijing National Laboratory for Molecular Sciences, State Key Laboratory of Rare Earth Materials Chemistry and Applications, College of Chemistry and Molecular Engineering, Peking University, Beijing 100871, P. R. China, Electron Microscope Lab, Peking University, Beijing 100871, P.R. China, and Intense Pulse Neutron Source Division, Argonne National Laboratory, Argonne, Illinois 60439

Received October 21, 2006. Revised Manuscript Received December 18, 2006

Titanium phosphate, $Na_3[Ti_2P_2O_{10}F]\cdot xH_2O$ (**1**), has been synthesized under hydrothermal conditions and structurally characterized using powder X-ray diffraction, neutron diffraction, and selected area electron diffraction (SAED). **1** crystallizes in the tetragonal space group *I*4/*mmm* with $a = 6.4207(1)$ Å and $c = 10.6762(2)$ Å and can be described by the stacking of a square-net sheet consisting of alternative linkage of $TiFO_5$ octahedra and PO_4 tetrahedra. The $TiFO_5$ octahedron is highly distorted, with a short "titanyl" Ti−O bond and a long Ti−F bond. The "titanyl" oxygen is almost doubly bonded to Ti; the square-net sheets are linked only by sharing common F atoms, which lead to a rather opened framework containing 2D channels in the *ab* plane. The counter cations Na^+ and water molecules reside in the channels. At high temperature, the adsorbed water molecules escape from the channels, leading to an anhydrous phase $Na_3[Ti_2P_2O_{10}F]$ (**2**) with exactly the same structural framework as that of **1**. **2** is stable at high temperature in an Ar atmosphere, but decomposes to other known titanium phosphates and oxide at about 650 °C in air. The Na ions in the compound are exchangeable. In addition, **2** exhibits a Na conductivity comparable to that of the NASICON type titanium phosphates (1.0×10^{-4} Ω^{-1} cm^{-1} at 200 °C).

Introduction

Titanium phosphates (TiPOs) are an interesting class of materials that may show various properties and applications, such as nonlinear optics,[1,2] ion exchange,[3] ion conductivity,[4] and redox catalysis.[5,6] In TiPO structures, Ti and P atoms are octahedrally and tetrahedrally coordinated and linked via sharing corners to form various frameworks. In the structure of KTP and related compounds $MTiOPO_4$ (M = Ag, Tl, Cs, Rb, K, Na, Li),[7] for example, the TiO_6 octahedra share corners to form octahedral chains; these are further interconnected by PO_4 tetrahedra, forming a 3D structure. The TiO_6 octahedron in the KTP structure is highly distorted with a short "titanyl" Ti−O bond (<1.75 Å) and a long *trans*-Ti−O bond (>2.1 Å). Such asymmetric trans bond distance is responsible for the localized bond polarization, which leads to large nonlinear optical coefficients. Another interesting family of TiPOs is the NASICON type $M^{I}Ti_2(PO_4)_3$ and the substituted series with a general formula $M^{I}_{1+x}Ti_{2-x-y}R^{III}_xR^{IV}_y(PO4)_3$, where M^{I} can be most of the alkaline metal ions and R^{III} and R^{IV} are the trivalent and tetravalent metal ions.[8−11] Most of the NASICON type TiPOs are good ionic conductors, particularly for Li^{I} and Na^{I} cations. In these structures, TiO_6 octahedra and PO_4 tetrahedra share corners and form 3D frameworks with small channels, within which the cations M^{I} are distributed and responsible for ionic conductivity. Partial substitution of Ti^{IV} by other trivalent ions may modify the concentration of the carries and their mobility, which may further modify ionic conductivity of the materials.

In the past several decades, a large number of new TiPOs with diverse structures ranging from 1D chains,[12,13] 2D layers[14−24] and even 3D open frameworks[25−29] have been synthesized. Most of them, however, are hydrated titanium

* Corresponding author. E-mail: liguobao@pku.edu.cn (G.L.); jhlin@pku.edu.cn (J.L.). Tel: (8610)62750342. Fax: (8610)62753541.
[†] Beijing National Laboratory for Molecular Sciences, Peking University.
[‡] Electron Microscope Lab, Peking University.
[§] Argonne National Laboratory.

(1) Masse, R.; Grenier, J. C. *Bull. Soc. Fr. Mineral. Cristallogr.* **1971**, *94*, 437−439.
(2) Satyanarayan, M. N.; Deepthy, A.; Bhar, H. L. *Crit. Rev. Solid State Mater. Sci.* **1999**, *24*, 103−191.
(3) Allulli, S.; Ferragina, C.; La Ginestra, A.; Massucci, M. A.; Tomassini, N. *J. Inorg. Nucl. Chem.* **1977**, *39*, 1043−1048.
(4) Delmas, C.; Nadiri, A. *Solid State Ionics* **1988**, *28*−*30*, 419−423.
(5) Serre, C.; Férey, G. *C. R. Acad. Sci., Ser. IIc* **1999**, *2*, 85−91.
(6) Ekambaram, S.; Serre, C.; Férey, G.; Sevov, S. C. *Chem. Mater.* **2000**, *12*, 444−449.
(7) Stucky, G. D.; Phillips, M. L. F.; Gier, T. E. *Chem. Mater.* **1989**, *1*, 492−509.
(8) Rodrigo, J. L.; Carrasco, P.; Alamo, J. *Mater. Res. Bull.* **1989**, *24*, 611−618.
(9) Arbi, K.; Lazarraga, M. G.; Chehimi, D. B.; Ayadi-Trabelsi, M.; Rojo, J. M.; Sanz, J. *Chem. Mater.* **2004**, *16*, 255−262.
(10) Patoux, S.; Rousse, G.; Leriche, J. B.; Masquelier, C. *Chem. Mater.* **2003**, *15*, 2084−2093.
(11) Maldonado-Manso, P.; Losilla, E. R.; Martinez-Lara, M.; Aranda, M. A. G.; Bruque, S.; Mouahid, F. E.; Zahir, M. *Chem. Mater.* **2003**, *15*, 1879−1885.
(12) Guo, Y. H.; Shi, Zh.; Yu, J. H.; Wang, J. D.; Liu, Y. L.; Bai, N.; Pang, W. Q. *Chem. Mater.***2001**, *13*, 203−207.
(13) Guo, Y. H.; Shi, Z.; Ding, H.; Wei, Y. B.; Pang, W. Q. *Chin. Chem. Lett.* **2001**, *12*, 373−376.
(14) Zhao, Y. N.; Zhu, G. S.; Jiao, X. L.; Liu, W.; Pang, W. Q. *J. Mater. Chem.* **2000**, *10*, 463−467.
(15) *Inorganic Ion Exchange Materials*; Clearfield, A., Ed.; CRC Press: Boca Raton, FL, 1982.

10.1021/cm062513w CCC: $37.00
Published on Web 01/24/2007

phosphates consisting of HPO_4 groups in the frameworks. Because the dehydration temperature of the HPO_4 group is rather low, the thermal stability of these hydrated titanium phosphates is, in general, low and thus hardly used in practice. Anhydrous frameworks of TiPOs can also be synthesized under hydrothermal conditions[30] by carefully tuning the reaction conditions. On the other hand, we have been attempting to synthesize new titanium borates (TiBOs), in particular, those with microporous framework structures, during the past several years. During the study, a new oxyfluorinated titanium phosphate $Na_3[Ti_2P_2O_{10}F]\cdot xH_2O$ (**1**) was obtained. Similar to the NASICON type structure, the framework of this compound also contains small channels in which Na cations and water molecules reside. At high temperature, water molecules can be completely removed, forming anhydrous $Na_3[Ti_2P_2O_{10}F]$ (**2**). The Na ions in the anhydrous compound are mobile and thus the material exhibits ionic conductivity and ion-exchange properties. In this paper, we report the synthesis, structure, conductivity, and ion-exchange properties of this material.

Experimental Section

Synthesis and Characterization. Single-phase samples of $Na_3[Ti_2P_2O_{10}F]\cdot xH_2O$ (**1**) were obtained under hydrothermal conditions in Teflon autoclaves starting from acidic suspensions of $NaBO_3\cdot 4H_2O$, $Ti(SO_4)_2$, and phosphoric acid in a molar ratio of 9.3:1.0:7.0 (Na:Ti:P). As a typical example, a mixture of 3.00 g (12.5 mmol) of $Ti(SO_4)_2$ (C.R.), 18.0 g (117mmol) of $NaBO_3\cdot 4H_2O$ (C.R.), and 6.0 mL (87.6mmol) of H_3PO_4 (85%), together with 6.0 mL of HBF_4(42%) and 10.0 mL of $NH_3\cdot H_2O$ (A.R.), was charged into a 50 mL Teflon-lined stainless steel autoclave. The autoclave was sealed, heated to 200 °C under autogenous pressure for 7 days, and then cooled to room temperature at a rate of 3 °C/h. About 2.50 g of product (yield 90% on the basis of $Ti(SO_4)_2$), appearing as white powder, was isolated by washing the product with hot distilled water and drying it at ambient temperature. **1** is stable and insoluble in water and most organic solvents. Initially, the synthetic study was aimed for titanium borates so that $NaBO_3\cdot 4H_2O$ was used in the starting materials. In fact, $NaBO_3\cdot 4H_2O$ can be replaced by NaH_2PO_4 without effecting the product. Other amines, such as triethylamine, ethylenediamine, or propane-1,3-diamine, can also be used in the reaction system. $Na_3[Ti_2P_2O_{10}F]$ (**2**) can be obtained by heating **1** at 700 °C in an Ar atmosphere.

Table 1. Recording Conditions of the MAS NMR Spectra

	^{1}H	^{19}F	^{31}P
chemical shift standard	TMS	$CFCl_3$	85%H_3PO_4
frequency (MHz)	399.7428	282.176	121.4
pulse width(μs)	1.5	10	1.2
flip angle	$\pi/2$	$\pi/2$	$\pi/2$
recycle time (s)	5	1	5
spinning rate (KHz)	25	7	6
no. of scans	8	300	400

The products were examined by X-ray diffraction on a Rigaku D/Max-2000 diffractometer. Powder X-ray diffraction data used for structure determination were recorded on a Bruker D8 Advance diffractometer with Cu $K_{\alpha 1}$ ($\lambda = 1.54056$ Å) radiation (2θ range, 10−120°; step, 0.0144°; scan speed, 60 s/step) at 50 kV and 40 mA at room temperature. The neutron diffraction data were collected at room temperature on the Special Environment Powder Diffractometer at the Intense Pulsed Neutron Source of Argonne National Laboratory. Selected area electron diffraction (SAED) and energy dispersive X-ray spectroscopy (EDX) were carried out on an H-9000 transmission electron microscope at 300 kV. Using EDX, we found fluorine in the compound with a 1.1:2.0 F:P ratio. The elemental ratio (Na:Ti:P) was measured by means of inductively coupled plasma optical emission spectroscopy (ICP-OES) on a Varian Vista RL spectrometer with radial plasma observation. As a typical analytic process, **1** was dissolved in acids (HCl or HCl plus HNO_3) to the appropriate concentration and then measured by ICP-OES for three parallel samples, which resulted in an average Na:Ti:P ratio of 1.55:1.00:1.05. Chemical analysis also confirms that the compound does not contain boron. Thermogravimetric−mass spectrometric analysis (TG−MS) was performed in a Netzsch STA 449C simultaneous analyzer utilizing Al_2O_3 crucibles and type-S thermocouples. The thermal stability was investigated up to 1073 K with TG−MS in a heating/cooling rate of 10 K/min in a dynamic argon atmosphere (gas flow, 0.03 L/min). The ^{1}H solid-state NMR spectrum was recorded on a Varian Unity Plus-400 spectrometer, ^{19}F and ^{31}P solid-state NMR on a Varian Unity Inova 300 spectrometer. The recording conditions of the spectra are listed in Table 1.

Structure Determination. The structure was determined by using an ab initio method on powder X-ray diffraction data. The powder diffraction data can be indexed[31] to a body centered tetragonal cell with $a = 6.4207(1)$ Å and $c = 10.6762(2)$ Å. The systematic absence of the reflections indicated the possible space groups, *I*4/*mmm*, *I*4*mm*, *I*$\bar{4}$2*m*, *I*$\bar{4}$*m*2, *I*422, *I*4/*m*, *I*$\bar{4}$ or *I*4. Figure 1 shows selective area electron diffraction (SAED) patterns in [001], [010], and [11$\bar{3}$] zones, which further confirm the I-centered tetragonal crystal system and the systematic absence of the reflections. To further determine the space groups, we conducted second-harmonic generation (SHG) coefficient measurements on powder samples by using the Kurtz−Perry method[32] with a YAG: Nd^{3+} laser (1064 nm). $Na_3[Ti_2P_2O_{10}F]\cdot xH_2O$ (**1**) does not show second order nonlinear optical effects, so the possible space group may be *I*4/*mmm* or *I*4/*m*.

The structure solution was initially established in the space group *I*4/*m* using the direct method,[33] where titanium, phosphorus, sodium,

(16) Christensen, A. N.; Andersen, A. G. K.; Andersen, I. G. K.; Alberti, G.; Nielsen, M.; Lehmann, S. M. *Acta Chem. Scand.* **1990**, *44*, 865−872.
(17) Bruque, S.; Aranda, M. A. G.; Losilla, E. R.; Olivera-Pastor, P.; Maireles-Torres, P. *Inorg. Chem.* **1995**, *34*, 893−899.
(18) Salvado, M. A.; Garcia-Granda, S.; Rodriguez, J. *Mater. Sci. Forum* **1994**, *166*−*169*, 619−624.
(19) Serre, C.; Taulelle, F.; Férey, G. *Solid State Sci.* **2001**, *3*, 623−632.
(20) Mafra, L.; Paz, F. A. A.; Rocha, J.; Espina, A.; Khainakov, S. A.; García, J. R.; Christian Fernandez, C. *Chem. Mater.* **2005**, *17*, 6287−6294.
(21) Liu, Y. L.; Shi, Z.; Fu, Y. L.; Chen, W.; Li, B. Z.; Hua, J.; Liu, W. Y.; Deng, F.; and Pang, W. Q. *Chem. Mater.* **2002**, *14*, 1555−1563.
(22) Li, Y. J.; Whittingham, M. S. *Solid State Ionics* **1993**, *63*−*65*, 391−395.
(23) Bortun, A. I.; Bortun, L. N.; Clearfield, A.; Villa-Garcia, M. A.; Garcia, J. R.; Rodriguez, J. *J. Mater. Res.* **1996**, *11*, 2490−2498.
(24) Serre, C.; Férey, G. *J. Mater. Chem.* **1999**, *9*, 579−584.
(25) Poojary, D. M.; Bortun, A. I.; Bortun, L. N.; Clearfield, A. *J. Solid State Chem.* **1997**, *132*, 213−223.
(26) Ekambaram, S.; Sevov, S. C. *Angew. Chem., Int. Ed.* **1999**, *38*, 372−375.
(27) (a) Fu, Y. L.; Liu, Y. L.; Shi, Z.; Zou, Y. C.; Pang, W. Q. *J. Solid State Chem.* **2001**, *162*, 96−102. (b) Liu, Y. L.; Shi, Z.; Fu, Y. L.; Chen, W.; Li, B. Z.; Hua, J.; Liu, W. Y.; Deng, F.; Pang, W. Q. *Chem. Mater.* **2002**, *14*, 1555−1563.
(28) Ekambaram, S.; Serre, C.; Férey, G.; Sevov, S. C. *Chem. Mater.* **2000**, *12*, 444−449.
(29) Liu, Y. L.; Shi, Z.; Zhang, L. R.; Fu, Y. L.; Chen, J. S.; Li, B. Z.; Hua, J.; Pang, W. Q. *Chem. Mater.* **2001**, *13*, 2017−2022.
(30) Serre, C.; Guillou, N.; Férey, G. *J. Mater. Chem.* **1999**, *9*, 1185−1189.
(31) Dong, C. *J. Appl. Crystallogr.* **1999**, *32*, 838.
(32) Kurtz, S. K.; Perry, T. T. *J. Appl. Phys.* **1968**, *39*, 3798−37813.

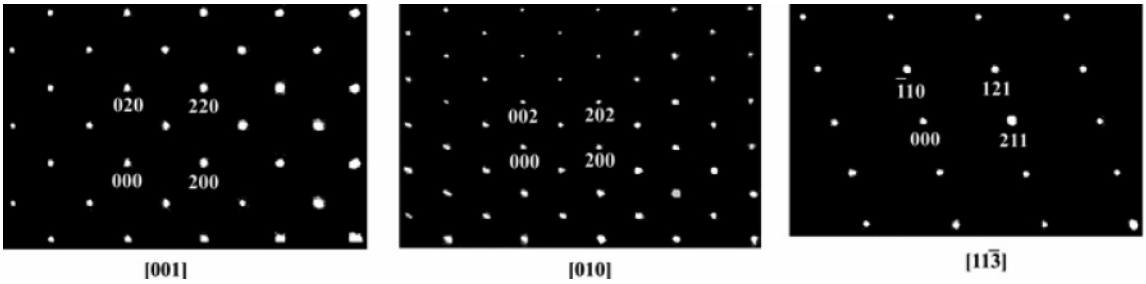

Figure 1. SAED patterns of $Na_3[Ti_2P_2O_{10}F]\cdot xH_2O$ (**1**).

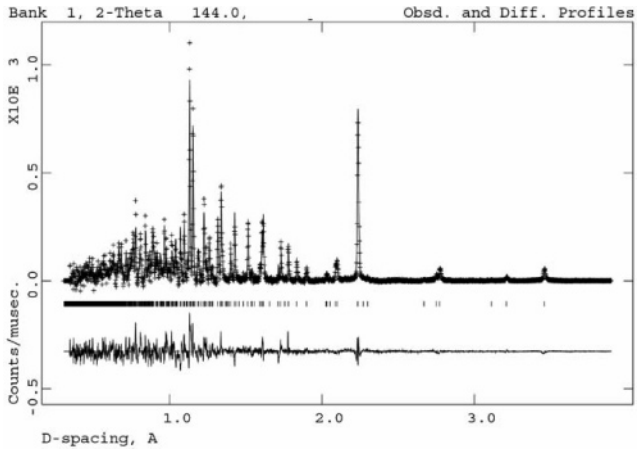

Figure 2. Rietveld fit of the powder neutron diffraction pattern for $Na_3[Ti_2P_2O_{10}F]\cdot xH_2O$ (**1**).

Table 2. Refined Structure Parameters and BVS Values for $Na_3[Ti_2P_2O_{10}F]\cdot xH_2O$ (1)[a]

atom	site	*x*, *y*, *z*	occupancy	BVS
Ti1	4e	0,0, 0.7993(1)	1	4.14
P1	4d	0, 0.5, 0.75	1	5.17
F1	2a	0, 0, 0	1	0.94
O2	4e	0, 0, 0.6484(1)	1	2.12
O3	16n	0, 0.3137(1), 0.8381(1)	1	2.04
Na/Ow1	8h	0.2782(1), 0.2782(1), 0	0.75/0.09	0.69

[a] Space group, *I*4/*mmm*; lattice constants, $a = 6.4207(1)$ Å, $c = 10.6762(2)$ Å; R factors, $R_P = 0.041$, $R_{wp} = 0.063$ for X-ray diffraction data; $R_P = 0.037$, $R_{wp} = 0.049$ for neutron diffraction data.

and part of the oxygen positions can be directly located. The rest of the oxygen positions were obtained by subsequent difference Fourier analysis.[34] Careful examining of the atomic parameters revealed that the structure can, in fact, be described in a higher-symmetry space group, *I*4/*mmm* (see the Supporting Information). The final structure refinement was carried out simultaneously on powder X-ray diffraction data and neutron diffraction data using the Rietveld method[35] with isotropic displacement parameters for all atoms. Figure 2 shows the profile fit of the neutron diffraction pattern. The refined atomic parameters and calculated bond valance sums are listed in Table 2. The fluorine atom (F1) was assigned on the basis of the result of EDX and the BVS value. Additionally, on the basis of the result of chemical analysis and charge balance, Na/Ow1 positions were occupied by Na ions with an occupancy factor of 0.75, the rest may be empty or filled by water molecules. While fixing the occupancy factor of Na ions to 0.75 and assuming that the water molecules are just located at the position of Na/Ow1, the refined occupation factor of water is about 0.09 for this particular sample.

Results and Discussion

Structure Description. The structure of $Na_3[Ti_2P_2O_{10}F]\cdot xH_2O$ (**1**) represents an interesting structure type consisting of $TiFO_5$ octahedra and PO_4 tetrahedra (Figure 3a). The Ti atom is located on the 4-fold axis of the structure and in a heavily distorted octahedron represented by a long Ti1−F1 bond (2.143(1) Å), a short Ti1−O2 bond (1.611(1) Å), and four regular Ti1−O3 bonds (2.056(1) Å). According to the BVS calculation, Ti1−O2 (BVS = 1.74) contains considerable double-bond character, which, similar to that observed in $MTiOPO_4$ (KTP),[7] could be considered as a titanyl Ti−O terminal bond in the framework. On the other hand, the site symmetry of *P*1 is $\bar{4}$; PO_4 thus adopts an ideal tetrahedral geometry with a P−O distance of 1.522(1) Å. Figure 3b shows a projection of the structure, and one can see that the structure can be conveniently described as repeat stacking of a square-net sheet along the *c* axis. Figure 3c shows the square-net sheet projected along the *c* axis, in which the $TiFO_5$ octahedra and PO_4 tetrahedra are alternatively linked via sharing four oxygen atoms (in the *ac* plane). Because of the geometry restriction of the PO_4 tetrahedron, the square-net sheet is buckled as shown in Figure 3b. In the square-net sheet, the doubly bonded O2 (the titanyl Ti1−O2 bond) is a terminal oxygen that does not contribute to the connection between the sheets. The square-net sheets are interconnected thereby only through sharing F atoms on $TiFO_5$ octahedra. Because of the long Ti−F−Ti distance (∼4.3 Å), the framework structure in **1** is quite open, containing 2-dimensional channels of 6-ring windows as shown in Figure 3b, which is topologically similar to $NaTi_2(PO_4)_3$[36] shown in Figure 3d. The Na ions are located within the channels and coordinated in a monocaped trigonal prism (Na−O2 = 2.563 (1) Å, Na−O3 = 2.496(1) Å, and Na−F = 2.526(1) Å).

NMR Spectroscopy. The ^{1}H MAS NMR spectrum of **1** contains a main peak at 5.3 ppm and two weak bands at about 10.0 ppm and 14.9 ppm, as shown in Figure 4a. The resonance peak at 5.3 ppm originates from physically absorbed water,[37] whereas the weak bands at 14.9 and 10.0 ppm may attribute to chemically adsorbed protons on the

(33) Altomare, A.; Burla, M. C.; Cascarano, G.; Giacovazzo, C.; Guagliardi, A.; Moliterni, A. G. G.; Polidiori, G. *J. Appl. Crystallogr.* **1995**, *28*, 842−846.
(34) Altomare, A.; Cascarana, G.; Giacovazzo, C.; Guagliardi, A. *SIRPOW User's Manual*; Inst. Di Ric. Per lo Sviluppo di Metodologie Cristallografiche, CNR: Bari, Italy.
(35) Larson, A. C.; von Dreele, R. B. *Report LAUR 86-748.*; Los Alamos National Laboratory: Los Alamos, NM, 1985.
(36) Rodrigo, J. L.; Carrasco, P.; Alamo, J. *Mater. Res. Bull.* **1989**, *24*, 611−618.
(37) Isobe, T.; Watanabe, T.; de la Caillerie, J. B. D.; Legrand, A. P.; Massiot, D. *J. Colloid Interface Sci.* **2003**, *261*, 320−324.

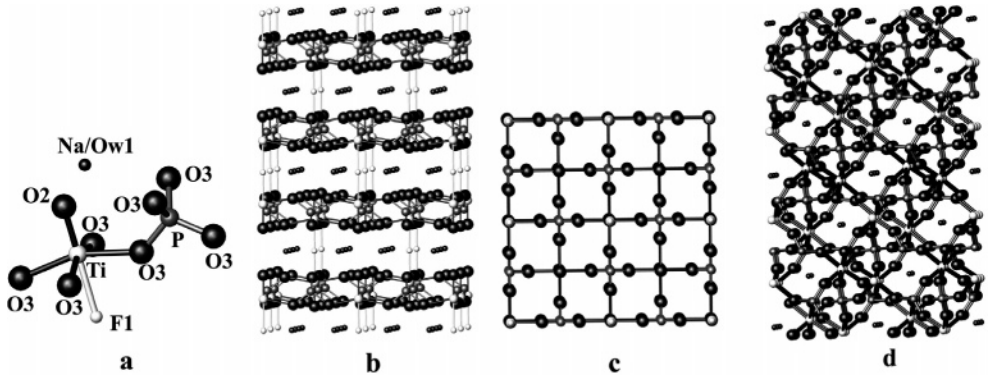

Figure 3. Sructure descriptions of $Na_3[Ti_2P_2O_{10}F]\cdot xH_2O$ (**1**): (a) the coordination geometries of Ti and P, (b) a projection of the structure, (c) the square-net sheet, and (d) a projection of $NaTi_2(PO_4)_3$[36] for comparison.

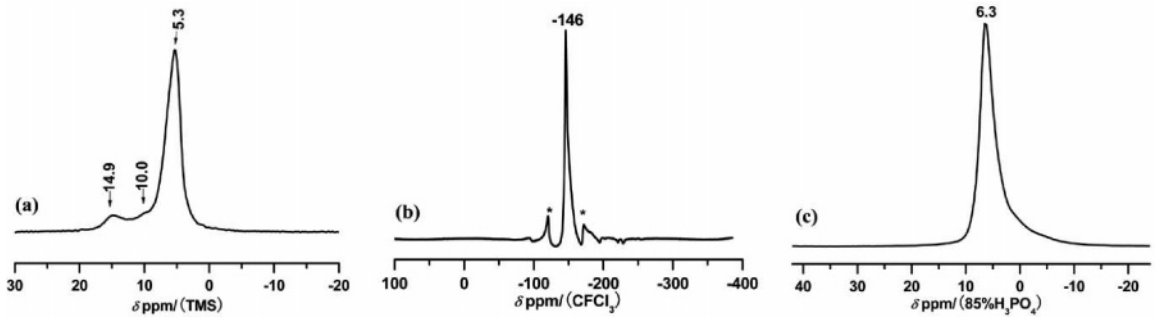

Figure 4. MAS NMR spectra of $Na_3[Ti_2P_2O_{10}F]\cdot xH_2O$ (**1**); (a) ^1H, (b) ^{19}F (* = spinning sidebands), and (c) ^{31}P.

surface of the sample, largely due to the formation of the $H_2PO_4^-$ or HPO_4^{2-} groups[38−40] on the surfaces of the particles. The peak at −146.0 ppm in the ^{19}F MAS NMR spectrum (reference $CFCl_3$; Figure 4b) originates from the bridging fluorine atom (Ti−F−Ti).[41,42] The resonance peak at 6.3 ppm in the ^{31}P MAS NMR spectrum (reference 85%H_3PO_4; Figure 4c) can be attributed to tetrahedrally coordinated P.[43−45] The MAS NMR spectra of ^1H, ^{19}F, and ^{31}P further confirm the presence of water molecules and fluorine atoms, as well as single crystallographic P site in the structure.

Thermal Stability. Figure 5 shows TG−MS curves of a sample of $Na_3[Ti_2P_2O_{10}F]\cdot xH_2O$ (**1**) in Ar. **1** loses weight gradually between 200 and 700 °C because of removal of the adsorbed water molecules in the channels. We also found that the content of the adsorbed water is slightly different in different samples (see the Supporting Information). X-ray diffraction patterns recorded after heat-treatment at different temperatures (Figure 6) show that the thermal stability of the framework is different in air and Ar. In air, the framework is retained up to about 650 °C, and above this temperature, it collapses and decomposes to $Na_4TiP_2O_9$,[46] $NaTiPO_5$,[47] and

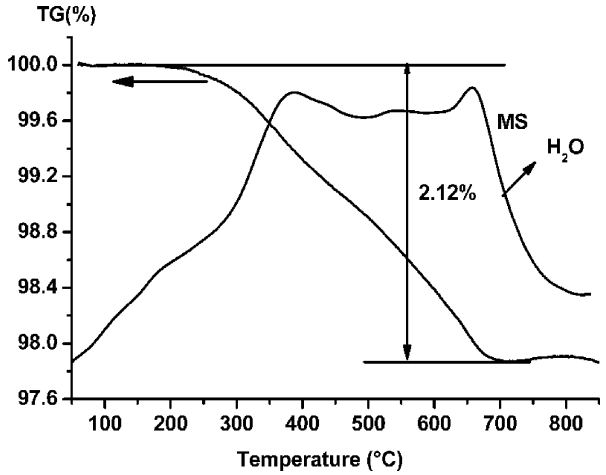

Figure 5. TG-MS curves of a $Na_3[Ti_2P_2O_{10}F]\cdot xH_2O$ (**1**) sample in an Ar atmosphere.

TiO_2.[48] In an Ar atmosphere, the framework may be maintained up to at least 800 °C, as shown in Figure 6. The low thermal stability of the compound in air originates from substitution of the fluorine atoms by oxygen, which results in the formation of the titanium phosphates and titanium oxide. Complete removal of the adsorbed water yields an anhydrous compound $Na_3[Ti_2P_2O_{10}F]$ (**2**). In Figure 7, we show a profile fit of neutron diffraction data collected after heat-treatment at 800 °C in Ar to the *I*4/*mmm* structure model. The atomic parameters of **2** (Table 3) show only a slight change from that of **1**. Therefore, the anhydrous compound adopts the completely same framework structure,

(38) Boysen, D. A.; Haile, S. M.; Liu, H. J.; Secco, R. A. *Chem. Mater.* **2003**, *15*, 727−736.
(39) Yamada, K.; Sagara, T.; Yamane, Y.; Ohki, H.; Okuda, T. *Solid State Ionics* **2004**, *175*, 557−562.
(40) Riou, D.; Fayon, F.; Massiot, D. *Chem. Mater.* **2002**, *14*, 2416−2420.
(41) Stamboulis, A.; Hill, R. G.; Law, R. V. *J. Non-Cryst. Solids* **2005**, *351*, 3289−3295.
(42) Loiseau, T.; Férey, G.; Haouas, M.; Taulelle, F. *Chem. Mater.* **2004**, *16*, 5318−5326.
(43) Taasti, K. I.; Christensen, A. N.; Norby, P.; Hanson, J. C.; Lebech, B.; Jakobsen, H. J.; Skibsted, J. *J. Solid State Chem.* **2002**, *164*, 42−50.
(44) Turner, G. L.; Smith, K. A.; Kirkpatrick, R. J.; Oldfield, E. *J. Magn. Reson.* **1986**, *70*, 408−415.
(45) Hartmann, P.; Vogel, J.; Schnabel, B. *J. Magn. Reson., Ser. A* **1994**, *111*, 110−114.
(46) Maximov, B. A.; Klokova, N. E.; Verin, I. A.; Timofeeva, V. A. *Kristallografia (Russ.)* **1990**, *35*, 847.
(47) Nagornyi, P. G.; Kapshuk, A. A.; Stus, N. V.; Slobobyanik, N. S. *Russ. J. Inorg. Chem.* **1989**, *34*, 1731.
(48) Meagher, E. P.; George, A. L. *Can. Mineral.* **1979**, *17*, 77.

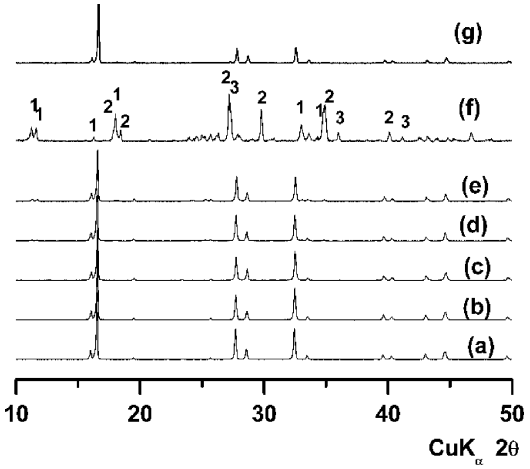

Figure 6. X-ray diffraction patterns of (a) an as-obtained $Na_3[Ti_2P_2O_{10}F]\cdot xH_2O$ (**1**) sample, a sample after heat-treatment for 12 h in air at (b) 200, (c) 500, (d) 600, (e) 650, (f) 800, and (g) a sample after heat-treatment at 800 °C for 12 h in an Ar atmosphere; the decomposition products are labeled as 1, $Na_4TiP_2O_9$; 2, $NaTiPO_5$; and 3, TiO_2.

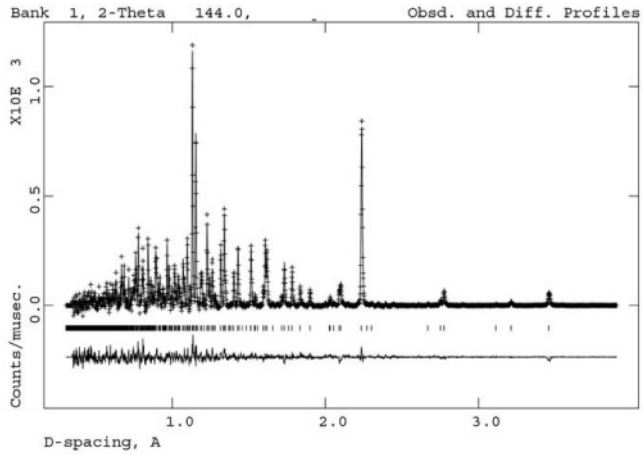

Figure 7. Rietveld fit of neutron diffraction of **2**, a sample after heat-treatment at 800 °C in an Ar atmosphere, to the structure model listed in Table 3.

Table 3. Refined Structure Parameters for $Na_3[Ti_2P_2O_{10}F]$ (2)[a]

atom	site	*x*, *y*, *z*	occupancy
Ti1	4e	0,0, 0.8015(1)	1
P1	4d	0, 0.5, 3/4	1
F1	2a	0, 0, 0	1
O2	4e	0, 0, 0. 0.6463(1)	1
O3	16n	0, 0.3079(1), 0.8353(1)	1
Na/Ow1	8h	0.2741(1), 0.2741(1), 0	0.75/0.0

[a] Space group, *I*4/*mmm*; lattice constants. a = 6.4208(1) Å, c = 10.6756(2) Å; R factors, R_P = 0.045, R_{wp} = 0.063.

and the only difference is that the adsorbed water molecules in the channels are completely removed, as indicated by the occupation factor of the Na/Ow1 site (0.75) in Table 3.

Ion Exchange. Ion-exchange reactions were carried out in aqueous solution at 60 °C. As a typical example, about 0.5 g of $Na_3[Ti_2P_2O_{10}F]\cdot xH_2O$ (**1**) was suspended and stirred in 75 mL of 1.0 mol LiCl solutions (pH ~7) for 24 h. After being filtered and washed with distilled water, the exchanged samples were examined by X-ray diffraction and chemical analysis (ICP-OES). The sample was then used for further ion exchange. Several other monovalant ions, such as K^+ and NH_4^+, were used in the exchange reaction, but only Li^+ was successfully substituted for Na^+ ions. The substitution

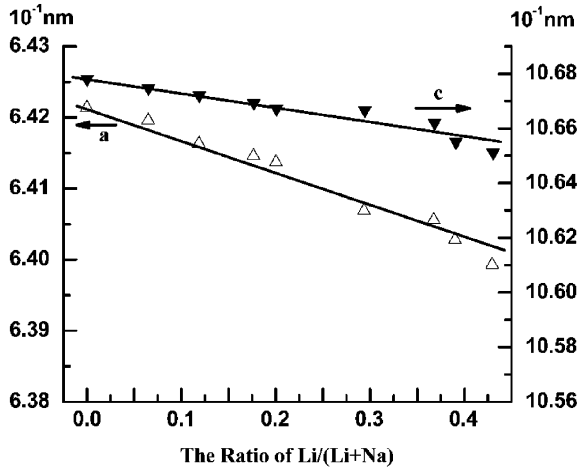

Figure 8. Correlation curve of the Li contents and the lattice constants a and c in $Na_{3-3y}Li_{3y}[Ti_2P_2O_{10}F]\cdot xH_2O$.

of Li for Na was confirmed by both chemical analysis and X-ray diffraction. Figure 8 shows the correlation of the measured Li content and the lattice constants for a series of samples, $Na_{3-3y}Li_{3y}[Ti_2P_2O_{10}F]\cdot xH_2O$. As the Li content in the sample increases, the lattice constants a and c decrease almost linearly, indicating that the Na ions in the channels were indeed exchangeable by Li ions.

Ionic Conductivity. AC impedance was measured with a HP4192A impedance analyzer with an ac voltage of 50 mV and frequency range of 5 Hz to 12 MHz between 200 and 540 °C. The samples were pressed into pellets and sintered at 700 °C for 20 h in an Ar atmosphere to remove the adsorbed water and obtain $Na_3[Ti_2P_2O_{10}F]$ (**2**). The density of the pellet estimated using the Archimedean method was about 90% of the ideal density. The electrode was painted with Pt paste on faces of the pellet and then treated at 550 °C for 30 min. Figure 9a is a typical impedance spectrum of **2** measured at 200 °C. The first semicircle represents bulk property, and the second semicircle, which is, in fact, overlapped with a straight line originating from the Warburg diffusion impedance,[49,50] is mainly caused by the grain boundary effect.[51] From the first semicircle measured at different temperatures, one could extract the bulk conductivity of the sample. The bulk conductivity data are plotted as $\log(\sigma T)$ vs $1000/T$ in Figure 9b. Intrinsic activation energies (E_a = 0.48 eV) were obtained from the slopes of the plot. The bulk conductivity value at 200 °C is about 1.0×10^{-4} Ω^{-1} cm^{-1}, which is comparable to that of NASICON type TiPOs[52] as shown in Figure 9b.

The charge carrier in the material is presumably the Na^+ ions in the channels of structure **2**. To confirm this, we constructed a concentration cell as shown below

$$\text{Pt NaCl}(c_0 = 0.1\text{ M}) \mid \text{Na}_3[\text{Ti}_2\text{P}_2\text{O}_{10}\text{F}] \mid \text{NaCl}(c_x)\text{ Pt} \quad (1)$$

Two aqueous NaCl solutions, one for reference and the other for measurement, were separated by solid electrolyte made

(49) Warburg, E. *Ann. Phys. Chem.* **1899**, *67*, 493.
(50) Macdonald, D. D. *Electrochim. Acta* **2006**, *51*, 1376.
(51) Abrantes, J. C. C.; Labrincha, J. A.; Frade, J. R. *Mater. Res. Bull.* **2000**, *35*, 955−964.
(52) Mouahid, F. E.; Bettach, M.; Zahir, M.; Maldonado-Manso, P.; Bruque, S.; Losilla, E. R.; Aranda, M. A. G. *J. Mater. Chem.* **2000**, *10*, 2748.

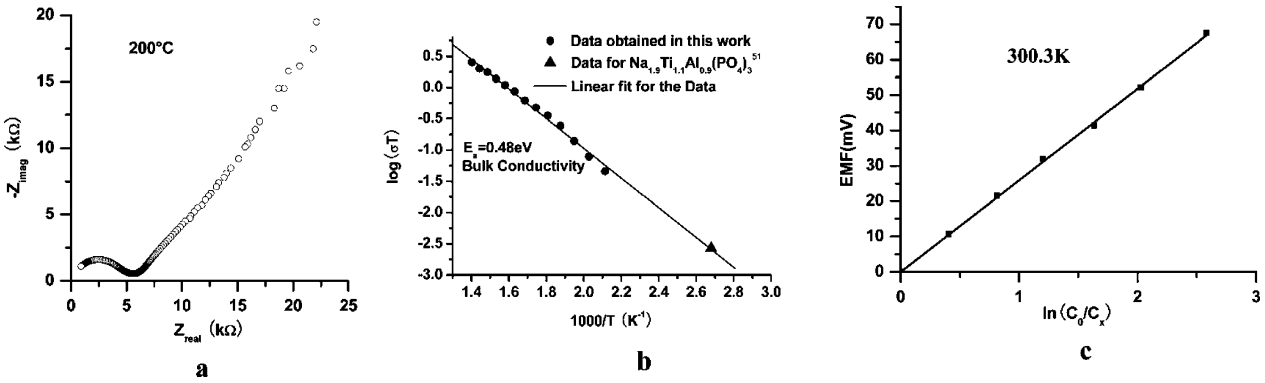

Figure 9. (a) Impedance spectrum of $Na_3[Ti_2P_2O_{10}F]$ (**2**) at 200 °C, (b) temperature dependence of the bulk conductivity, and (c) dependence of the EMF on the concentration of NaCl at 300.3(1) K for a concentration cell shown in eq (1).

by $Na_3[Ti_2P_2O_{10}F]$ (**2**). Grid Pt films on both surfaces of the pellet were used as electrodes, and two bended glass tubes were then bonded on both surfaces, in which the reference and measured solutions were added. For dilute solution (C_x is less than 0.1 M), the potential of the concentration cell follows

$$E = t_{ion}(RT/nF)\ln(C_0/C_x) \quad (2)$$

where E is the electromotive force (EMF) of the cell; t_{ion}, the ionic transference number; R, the gas constant; T, the temperature; n, the charged number of the ion (for Na^+ here, $n = 1$); and F, the Faraday constant. The EMF was measured by using a UJ37 potentiometer. As shown in Figure 9c, the EMF of the cell shows a linear dependence on $\ln(C_o/C_x)$ with a measured transference number of Na^+ close to 1.0, indicating that the charge carriers in the material are sodium ions.

Conclusion

A new titanium phosphate $Na_3[Ti_2P_2O_{10}F]\cdot xH_2O$ (**1**) has been synthesized by the hydrothermal method. At high temperature, the adsorbed water molecules in **1** can be completely removed to form an anhydrous phase, $Na_3[Ti_2P_2O_{10}F]$ (**2**), with an identical framework structure. The framework structures in **1** and **2** can be described as repeat stacking of a square-net sheet. The square-net sheet is rather similar to the (100) perovskite layer, where half of the octahedra are replaced by PO_4 tetrahedra in an alternative fashion; each $TiFO_5$ octahedron thus connects to four PO_4 tetrahedra in the plane, and vice versa, in the square-net sheet. Such a square-net was also observed in other layered titanium phosphates, such as $Ti_2(PO_4)_2F_4\cdot C_2N_2H_{10}$ and $Ti_2(PO_4)_2F_4\cdot C_3N_2H_{12}\cdot H_2O$.[24] The octahedron TiF_2O_4 shares four oxygen atoms with PO_4 in the plane and leaves two axial fluorine atoms as terminal atoms, so that these are layered compounds. A similar square-net was also observed in another layered compound, $VOPO_4\cdot 2H_2O$.[53] This square-net sheet might be considered as an extreme asymmetric example, in which the vanadium ions are coordinated in square pyramidal geometry with a short double terminal V═O bond and four regular V−O bonds to the PO_4 groups. In **1** and **2**, the $TiFO_5$ octahedra are also highly asymmetric, with an opposite axial short Ti−O2 (1.611(1) Å) and long Ti−F1 (2.143(1) Å) distances. However, the square-net sheets are interconnected via the fluorine atom and thus form a 3D framework. Additionally, unlike the perovskite structure, the framework is rather open, containing 6-ring windows within the *ab* plane, in which the sodium ions and water molecules reside.

The sodium cations in $Na_3[Ti_2P_2O_{10}F]\cdot xH_2O$ are exchangeable. Although only Li^+ was successfully exchanged into the material in present study, this is does not mean that the large alkaline ions, such K^+ and NH_4^+, are not exchangeable; we would rather attribute this observation to the kinetic reason, because even for Li^+, the exchange reaction was quite slow under present conditions (60 °C in aqueous solution). At high temperature, the adsorbed water molecules escape from the channels, yielding anhydrous $Na_3[Ti_2P_2O_{10}F]$ (**2**). The framework structure in **2** is completely the same as that in **1**, in which the Na/Ow1 site is partially occupied by only Na ions. Therefore, $Na_3[Ti_2P_2O_{10}F]$ (**2**) is rather similar to NISICON type TiPOs as far as the mobility of the counter cations is concerned. The conductivity of $Na_3[Ti_2P_2O_{10}F]$ (**2**) is moderate, which is similar in magnitude to that of the NISICON compound $Na_{1+x}Ti_{2-x}Al_x(PO_4)_3$,[52] as is the activation energy ($E_a = 0.48$ eV). Although considering that our preliminary conductivity study was conducted only on stoichiometric $Na_3[Ti_2P_2O_{10}F]$ and, additionally, that this material behaves as a pure ionic conductor, further modification of the materials is desired to improve the conductive properties.

Acknowledgment. We thank Dr. Guiling Wang (research and application of tunable all-solid-state laser of Key Laboratory of Optical Physics, Institute of Physics, Chinese Academy of Sciences) for the help measuring the NLO effects of **1**. This work is supported by the National Natural Science Foundation of China (Grants 20471003 and 20531010).

Supporting Information Available: X-ray crystallographic file in CIF format, calculated and observed X-ray diffraction pattern, the details of the structure determination, thermogravimetric analysis diagram for **1**. This material is available free of charge via the Internet at http://pubs.acs.org.

(53) Tietze, H. R. *Aust. J. Chem.* **1981**, *34*, 2035.

CM062513W